ORIGINAL PAPER

CrossMark

Estimation of the thermal and photochemical stabilities of pheromones

F. N. Tomilin [1,2] · A. S. Fedorov [1,2] · P. V. Artyushenko [3] · S. G. Ovchinnikov [1,2] · T. M. Ovchinnikova [4] · P. E. Tsikalova [3] · V. G. Soukhovolsky [4]

© Springer-Verlag GmbH Germany, part of Springer Nature 2018

Abstract

The correlation between the kinetic stability of molecules against temperature and variations in their geometric structure under optical excitation is investigated by the example of different organic pheromone molecules sensitive to temperature or ultraviolet radiation using the density functional theory. The kinetic stability is determined by the previously developed method based on the calculation of the probability of extension of any structural bond by a value exceeding the limit value L_{Max} corresponding to the breaking of the bond under temperature excitation. The kinetic stability calculation only requires the eigenfrequencies and vibrational mode vectors in the molecule ground state to be calculated, without determining the transition states. The weakest bonds in molecules determined by the kinetic stability method are compared with the bond length variations in molecules in the excited state upon absorption of light by a molecule. Good agreement between the results obtained is demonstrated and the difference between them is discussed. The universality of formulations within both approaches used to estimate the stability of different pheromone molecules containing strained cycles and conjugated, double, and single bonds allows these approaches to be applied for studying other molecules.

Keywords Kinetic stability · Atomic structure · Density functional theory · Excited states · Terpenes

Introduction

The transmission of information by insects is carried out with the help of special odorous substances called pheromones [1]. For most insects, pheromones consist of several components, belonging to different classes of substances. For example, moths of the family Geometridae of the insect order Lepidoptera use as pheromone unsaturated straight-chain hydrocarbons containing 17–21 carbon atoms or their oxygen-containing derivatives (Fig. 1a), for xylophagous insects of the order Coleoptera most of the compounds belong to the group of terpenes and terpenoids (Fig. 1b).

The stability of pheromone molecules, i.e., their lifetime under the action of external factors, including irradiation, heating, and chemical interaction with air components, determines, to a great extent, the efficiency of insect chemical communication. The pest insect population fecundity on the one hand, and the beneficial insect population decline on the other hand, determine the importance of universal theoretical methods for estimating the effect of external factors on insect chemical communication based on recognition of pheromone molecules by insects of the opposite sex before the decay of such molecules under ultraviolet (UV) optical irradiation and heating. Due to the huge diversity of insect species using multicomponent mixtures of organic compounds as pheromones, the lifetime of such molecules should be estimated using theoretical techniques [4–9], since the experimental investigations of the properties of pheromone molecules known to date are nearly impossible.

In [9], we studied the effect of humidity and light on pheromone molecules of xylophage insects using the density functional theory (DFT) calculations based on the B3LYP method.

✉ F. N. Tomilin
felixnt@gmail.com

1 Kirensky Institute of Physics, Federal Research Center KSC SB RAS, Krasnoyarsk 660036, Russia

2 Siberian Federal University, Krasnoyarsk 660041, Russia

3 Federal Research Center KSC SB RAS, International Scientific Center for Extreme Organism States Research, Krasnoyarsk 660036, Russia

4 Sukachev Institute of Forest, Federal Research Center KSC SB RAS, Krasnoyarsk 660036, Russia
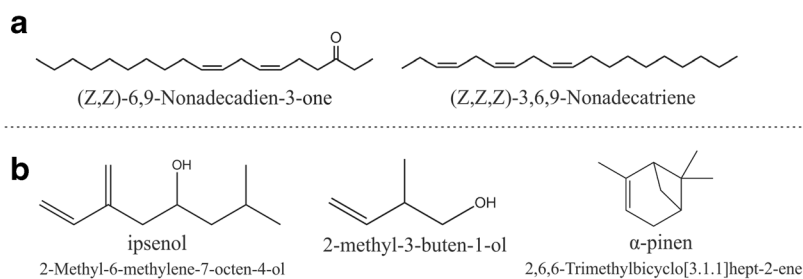
Fig. 1 **a** Pheromone of the willow beauty *Peribatodes rhomboidaria* Denis & Schiffermüller, moth of the family Geometridae of the insect order Lepidoptera [2]; **b** Pheromone of the black pine beetle *Monochamus galloprovincialis* Oliv., xylophagous insect of the order Coleoptera [3]

In the present work, we estimate the temperature stability of pheromone molecules using the nanostructure kinetic stability (KS) technique proposed by us in [10, 11] and successfully applied for estimating the KS and experimental yield of molecules of different fullerenes and carbon nanotubes [10] and simple saturated hydrocarbon molecules [11]. The insect pheromone molecules, which have a limited lifetime and are easily destructed by external factors, can serve as references for testing our KS calculation technique. To perform the complex estimation of the stability of different pheromone classes against temperature and light, we compared the probabilities of breaking of the weakest bonds in molecules and their lengths calculated using the KS technique, as well as the variations in the geometry of molecules under light excitation.

Experimental

Here, we employ our theoretical kinetic stability (KS) model, which was proposed first and applied to studying some fullerenes and carbon nanotubes in [10]. The model is based on calculating the probability of nanostructure bond breaking via determining the normal vibrational modes and using the central limit theorem. The main features of the initial KS model were described in detail in the Supporting information, part **S**1. The normal vibrational modes were found using the force matrix calculations and the subsequent calculations of all vibrational eigenvalues and eigenvectors. According to the KS model, the probability P_{destr} of the molecule's weakest bond breaking corresponds to the molecule lifetime: the high probability is indicative of the short lifetime of the molecule and vice versa. Alternatively, the high or low value of the inverse quantity P_{destr}^{-1} is indicative of the high or low molecule's lifetime, respectively.

Here, we only point out that the KS is based on the assumption that the extension of any chemical bond connecting two atoms is a joint result of the effect of a great number of vibrational modes, with each mode making a minor contribution to the displacement of the atoms connected by the bond. Under these conditions, it is reasonable to use the central limit theorem (CLT) of statistics. Using the CLT, we can calculate the probability of the bond breaking P_{destr} when the bond between atoms n and m is

broken if the change of bond length $\Delta \overrightarrow{R}(n, m, t) > X_{max}$, where X_{max} is the maximum bond length. At that the probability of the bond breaking can be written as:

$$P_{destr} = P(\Delta R(n, m, t) \geq X_{max})$$

$$= \frac{2}{\sqrt{\pi} s_n(n, m)} \int_{X_{max}}^{\infty} e^{-\frac{u^2}{2 s_n^2(n,m)}} du$$

$$= {}^1/_2 \, erfc \left(\frac{X_{max}}{\sqrt{2} s_n(n, m)} \right), \qquad (1)$$

where $erfc(x) = 1 - erf(x)$, $erf(x)$-error function, and the total variance $s_N^2(n, m) = \sum_{k=1}^{n} \sigma_k^2(n, m)$ for (n,m) pair is the sum of variances over all the vibrational modes k, which can be easily calculated using the vibrational mode eigenvector k and eigenvalues and temperature T.

The maximum chemical bond extension in all the calculations was taken to be $L_{Max} = X_{Max} - L_0 = 0.98A$, where L_0 is the equilibrium bond length. This value L_{Max} was determined in our work [10] devoted to the KS calculations of some small linear hydrocarbon and benzene molecules at high temperatures. The L_{Max} value was determined by fitting of the molecule total energy (U(r)) profile under the bond extension by the quadratic function. The KS values predicted by our model were found to be qualitatively consistent with the relative experimental abundance of some fullerenes and nanotubes of different chiralities. Here, we present the KS model, which was applied to some pheromone molecules.

The pheromone molecule geometry was optimized by the quantum chemical DFT technique using the B3LYP method [12–14] in the cc-pVDZ basis of the GAMESS program [15]; after that, the KS was analyzed via calculating the Hessian for the molecule ground state. To estimate the most probable changes in the geometry of molecules under photoexcitation, we optimized the geometry in the excited state by the time-dependent TD/B3LYP/cc-pVDZ technique [16, 17]. The B3LYP functional is one of the most popular; it yields good agreement between the calculated parameters of organic compounds and the experiment [18–21]. The correlation consistent cc-pVDZ basis set allows one to correctly describe bond lengths, valence angles, dipole moment, electron density

distribution, and other structural and spectral characteristics of organic molecules [22, 23].

The structure of natural molecules can be affected by temperature and solar radiation. The terpene molecules exposed to the UV radiation can pass to the excited state; in this case, the bond lengths and valence angles in molecules change, the bonds can break, and the molecular cycles can open. After that, the modified molecules can further transform to a new substance [24]. The stability of molecules against various external factors can be estimated using the approach based on quantum-mechanical calculations.

Most compounds belong to the terpene and terpenoid groups [25–27] related to the resin odorous substances. The species specificity of terpenes is determined by the structural and optical isomers. The geometrical parameters of molecules (Fig. 2) do not allow atoms to freely exchange by their positions and, consequently to form different conformers. For the investigations, we chose pheromones of three xylophage insect species, which are dangerous for forest, specifically, bark beetles *Ips typographus* L., black fir tree beetles *Monochamus urussovi* Fish., and black pine beetles *Monochamus galloprovincialis* Oliv. belonging to the Coleoptera order. The complex and diverse structure of the Coleoptera pheromones (Fig. 2) allowed us to analyze the applicability of the KS technique for different chemical compounds.

The *Ips typographus* pheromone contains 2-methyl-3-buten-2-ol, cis-verbenol, trans-verbenol, 2-phenyl-ethanol, myrtenol, and trans-myrtenol. The *Monochamus urussovi* pheromone contains five substances without oxygen-bearing ones: 1S-alpha-pinene, 1R-alpha-pinene, S-3carene, R-limonene, and alpha-terpinolene. The *Monochamus galloprovincialis* pheromone consists of the three main components: ipsenol, α-pinen, and 2-methyl-3-buten-1-ol [3, 28–34]. Systematic names of pheromone molecules are given in Table 1.
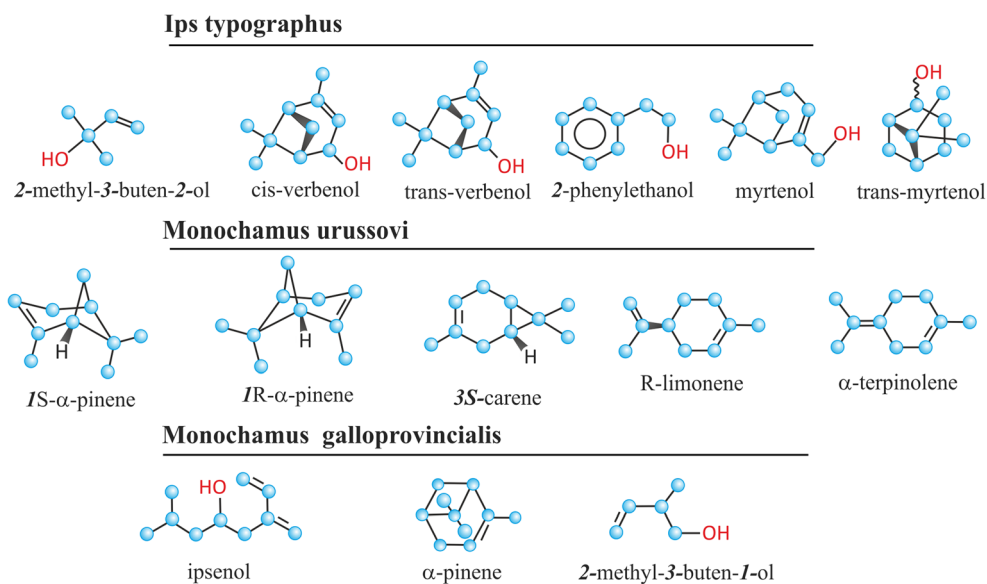
Results and discussion

To analyze the effect of temperature on the pheromone structure, we divided the molecules of the chosen insects into three groups (Fig. 3) according to their structural type: acyclic (group I), monocyclic (group II), and bicyclic (group III). The data obtained by calculating the temperature effect on the atomic structure of pheromone molecules were compared with the calculated data on the effect of light. To analyze the effect of temperature on the stability of different pheromone molecules, we calculated the effective frequencies of breaking of the weakest bonds in a molecule. To do this, we used Eq. (1) for calculating the probabilities of breaking of each bond in a molecule, i.e., the probabilities of the fact that the change in the bond length in a molecule exceeds the "maximum" bond extension $L_{Max} = 0.98$ A.

Table 1 (second column) gives the probabilities of breaking of the weakest bonds in a molecule under heat fluctuations for different pheromone classes. All the probabilities are normalized to the probability of breaking of the weakest bond (the probability of its breaking is given in parenthesis). The table data are given for the bonds with the breaking probability of no less than 0.01 of the probability of breaking of the weakest bond. The normalized probabilities of breaking of the weakest double bonds in a molecule are marked with the asterisk. The calculated temperature effect (second column) on the pheromone molecule geometry is compared with the calculated effect of light. The equilibrium lengths of the calculated weakest bonds are given in the third column.

The fifth column gives the bond length variations for the corresponding molecule after its photoexcitation. Sign + indicates the increase in the bond length after photoexcitation of a molecule; negative values indicate the decrease in the bond length. The rightmost column shows whether the bond length variations in the excited state coincide with the data of analysis of vibrations.

Fig. 2 *I.typographus, M.urussovi,* and *M.galloprovincialis* xylophage insect pheromones. Carbon atoms are marked in blue

Ips typographus

2-methyl-3-buten-2-ol   cis-verbenol   trans-verbenol   2-phenylethanol   myrtenol   trans-myrtenol

Monochamus urussovi

1S-α-pinene   1R-α-pinene   3S-carene   R-limonene   α-terpinolene

Monochamus galloprovincialis

ipsenol   α-pinene   2-methyl-3-buten-1-ol

Table 1 Variations in the structural characteristics of molecules under temperature and photoexcitation

Number of carbon atoms	Temperature excitation		L*, Å	Photoexcitation		Coincidence of the calculated KS and excited state
	normalized (absolute) fracture frequency, dimensionless value			$^{+}L_{ex}$, Å	$\Delta L^{\&}$, Å	
Group I						
2-methyl-3-buten-2-ol						
2–3	1		1541	1645	+0.104	coincide
1–2	0.75		1540	1541	+0.001	not coincide
#5–4	1.958e − 051		1.330	1445	+0.111	coincide
2methyl-3buten-1ol						
3–4	1.00		1541	1533	−0.008	not coincide
3–5	0.60		1535	1541	+0.006	not coincide
#2–1	1.5618e − 049		1338	1404	+0.066	coincide
*Ipsenol						
**2-Methyl-6-methylene-7-octen-4-ol						
4–5	1.00		1559	1551	−0.008	not coincide
5–6	0.01		1525	1426	−0.099	coincide
5–7	0.05		1560	1600	+0.040	coincide
#22–24	1.1612e − 053		1341	1383	+0.042	coincide
#8–23	1.2791e − 051		1345	1323	−0.022	coincide
Group II						
2-phenyl-ethanol						
7–8	1		1530	1539	+0.009	coincide
#5–6	4.7729e − 021		1403	1436	+0.033	coincide
#4–3	3.5389e − 023		1.397	1425	+0.028	coincide
#2–1	4.7371e − 023		1.397	1430	+0.033	coincide
Alpha-terpinolene						
1-Methyl-4-(1-methylethylidene)-cyclohexene						
5–7	1.00		1539	1580	+0.041	coincide
4–6	0.03		1520	1482	−0.038	not coincide
#8–9	1.6461e − 046		1342	1437	+0.095	coincide
#2–4	2.7368e − 042		1352	1424	+0.072	coincide
R-lemonen						
(R)-1-Methyl-4-(1-methylethenyl)-cyclohexene						
2–5	1.00		1546	1542	−0.003	not coincide
1–2	0.01		1536	1537	+0.001	not coincide
#3–4	1.1358e − 047		1343	1419	+0.076	not coincide
#8–19	2.3943e − 048		1341	1447	+0.106	not coincide
Group III						
Trans-mytrenol						
(1S,5R)-6,6-Dimethylbicyclo[3.1.1]heptan-2-ol						
3–7	1		1574	1573	−0.001	not coincide
1–7	0.92		1571	1541	−0.030	not coincide
2–3	0.01		1559	1557	−0.002	coincide
5–1	0.007		1540	1856	+0.318	coincide
Cis-verbenol						
cis-4,6,6-Trimethylbicyclo[3.1.1]hept-3-en-2-ol						
1–6	1		1583	2633	+1050	coincide
Mytrenol						
6,6-Dimethylbicyclo[3.1.1]hept-2-en-2-yl-methanol						
2–8	1		1584	2646	+1062	coincide

Table 1 (continued)

Number of carbon atoms	Temperature excitation		L*, Å	Photoexcitation		Coincidence of the calculated KS and excited state
	normalized (absolute) fracture frequency, dimensionless value			$^{+}L_{ex,}$ Å	$\Delta L^{\&}$, Å	
8–6	0.03		1577	1489	−0.088	coincide
Trans-verbenol						
(1S,5R)-6,6-Dimethylbicyclo[3.1.1]heptan-2-ol						
1–6	1		1586	1670	+0,084	coincide
#3–2	7.8559e − 053		1344	1434	+0.090	coincide
Alpha-pinene						
2,6,6-Trimethylbicyclo[3.1.1]hept-2-ene						
6–7	1		1583	2777	+1194	coincide
#4–5	8.8800e − 053		1344	1421	+0.077	not coincide
1R-alpha-pinene						
(1R,5R)-2,6,6-Trimethylbicyclo[3.1.1]hept-2-ene						
1–2	1.00		1583	2721	+1138	coincide
1–4	0.01		1576	1485	−0.091	not coincide
1S-alpha-pinene						
(1S)-2,6,6-Trimethylbicyclo[3.1.1]hept-2-ene						
5–6	1.00		1583	2835	+1252	coincide
4–6	0.02		1576	1480	−0.096	coincide
3S-caren						
(1S)-3,7,7-Trimethylbicyclo[4.1.0]hept-3-ene						
3–6	1.00		1517	1825	+0.308	coincide
3–7	0.04		1523	1499	−0.024	coincide
5–4	0.02		1545	1543	−0.002	coincide
6–7	0.08		1524	1505	−0.019	coincide

* trivial name

** systematic name,

is double bond,

+ is the increase in the bond length under photoexcitation, and

– is the decrease in the bond length under photoexcitation;

L*, Å is the bond length in the ground state in angstrom;

$^{+}L_{ex}$, Å is the bond length in a molecule in the excited state in angstrom;

$\Delta L^{\&}$, Å is the difference between the bond lengths in the ground and excited states in angstrom.

Analysis of the vibrational modes allowed us to estimate the role of temperature in the breaking of chemical bonds. The calculated excited state of molecules makes it possible to characterize the effect of solar radiation on the pheromone structure. The group-I acyclic molecules 2-methyl-3buten-2-ol (Fig. 3 I-a, I-b) and 2-methyl-3-buten-1-ol (Fig. 3 I-c, I-d) contain one double bond each; the strongest structural variations under excitation of molecules are observed in the multiple bond region. In the ipsenol molecule (Fig. 3 I-e, I-f) containing a system of conjugated double bonds, the structural changes in the multiple bond region under excitation are not stronger than the changes in the single bond length. As expected, the Hessian analysis did not show significant vibrations of double bonds, unlike the case of single bonds. Therefore, upon vibrations, the bonds with the maximum length can easily break. In the 2-methyl-3-buten-1-ol molecule, the change in the C2-C3 bond length comparable with the change in the double bond length coincides with the place of the most probable structural changes in the analysis of vibrations (Table 1). In the ipsenol molecule, the strongest changes in the length of single bonds in the structure also coincided with the calculated Hessian data, although the probability of variations in the C5-C6 and C5-C7 bond lengths is lower than the probability of variations in the C4-C5 bond length (Table 1).

Carbon atoms are marked in blue, oxygen atoms are marked in red, hydrogen atoms are marked in gray.

Group 2 includes monocyclic pheromone molecules. In the 2-phenyl-ethanol molecule, the strongest change in the bond length under excitation is observed between atoms C7-C8
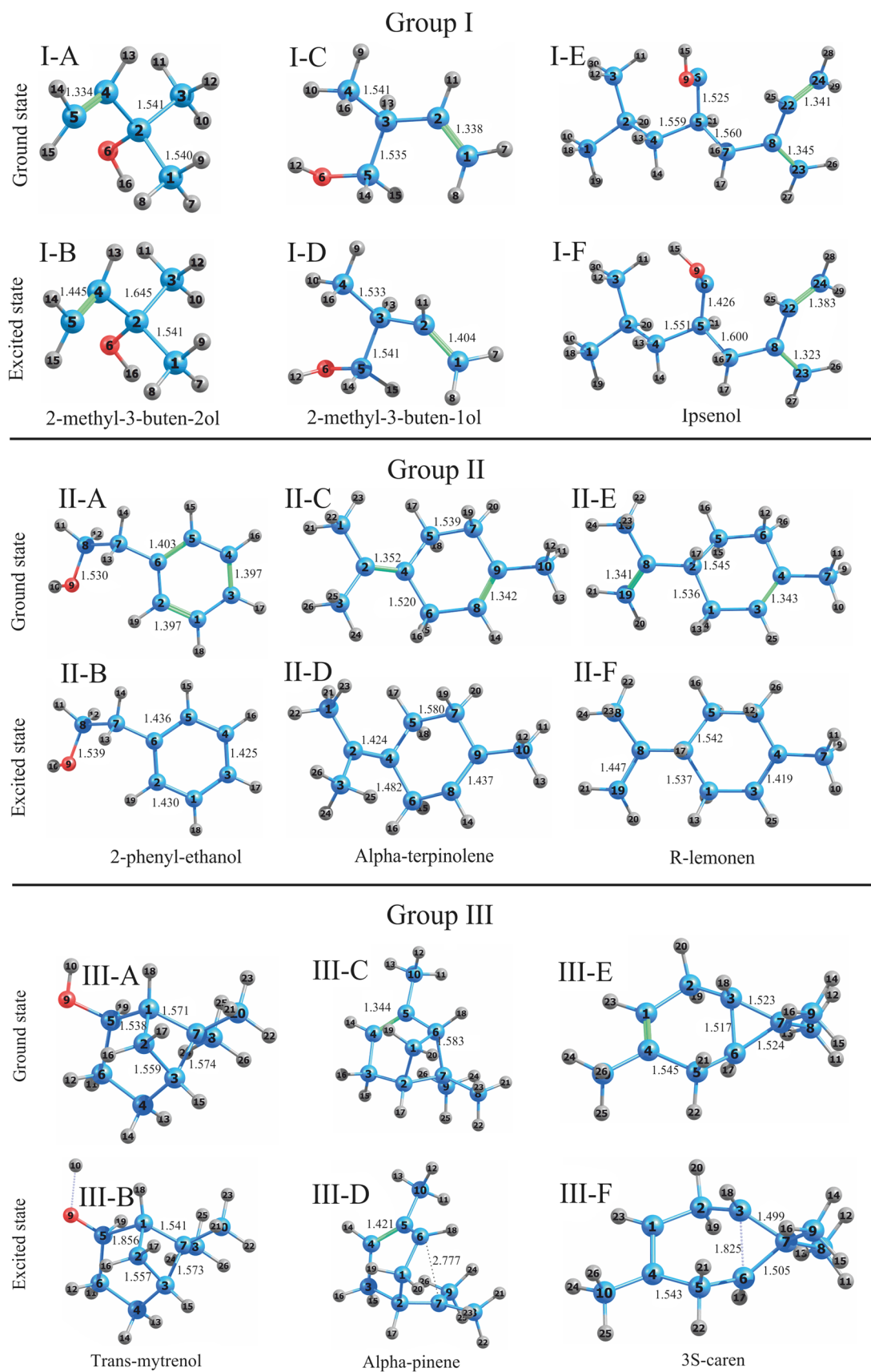
Fig. 3 Atomic structure of xylophage pheromone molecules in the ground and excited states. Group 1 includes acyclic molecules; group 2, monocyclic molecules; and group 3, bicyclic molecules

(Fig. 3 II-a, II-b); the temperature effect also changes the C7-C8 bond the most (Table 1). After absorption of the light quantum, the bonds inside the benzene ring of the 2-phenyl-ethanol molecule slightly change (Fig. 3 II-b), while the temperature excitation does not affect the benzene ring. In alpha-terpinolene (Fig. 3 II-c, II-d) containing two isolated double bonds, both the photo- and temperature excitations change the length of the single C5-C7 and C4-C6 bonds included in the hexatomic cycle. The C5-C7 bond increases by 0.041 A and the C4-C6 bond decreases by 0.038 A (Table 1). The strongest change in the bond length after absorption of light is observed for the double C2-C4 bond, which is not included in the cycle (Fig. 3 II-d). In the R-lemonen molecule (Fig. 3 II-e, II-d), the temperature excitation will, most probably, lead to the change in the lengths of single C2-C5 and C1-C2 bonds included in the cycle, while the photoexcitation does not change the length of these bonds (Table 1). Absorption of light leads to the extension of double bonds by 0.076 A inside the cycle and by 0.106 A beyond it. Similar to the case of acyclic phero-mone molecules, the absorption of light in cyclic molecules changes most strongly the structure of multiple bonds, while the heat radiation affects single bonds.

Group 3 consists of bicyclic pheromone molecules. Figure 3 shows only three molecules of this type. Since the structural variations in the alpha-pinene, cis-verbenol, mytrenol, trans-verbenol, 1R-alpha-pinene, and 1S-alpha-pinene molecules under irradiation are similar, Fig. 3 only shows the alpha-pinene molecule.

The thermal vibrations in the trans-mytrenol molecule (Fig. 3 III-a, III-b) will most probably lead to the breaking of the C3-C7 and C7-C1 bonds included in both the tetratomic and hexatomic cycle. Since the initial C3-C7 bond length is 1.573 A and the C1-C7-C3 angle is 85° instead of the angle 109° typical of the sp^3-hybridized orbitals, we may assume that the change in the bond length is related to the breaking of one of the bonds and opening of the strained tetratomic cycle. Upon radiation absorption, the C5-C1 bond included only in the hexatomic cycle extends by 0.318 A. Photoexcitation will, most likely, lead to the opening of the hexatomic cycle, while the tetratomic cycle remains invariable, in contrast to the case of the temperature effect (Table 1).

In the alpha-pinene (Fig. 3 III-c, III-d), cis-verbenol, mytrenol, trans-verbenol, 1R-alpha-pinene, and 1S-alpha-pinene molecules, the maximum elongations of a single bond included in the hexatomic and tetratomic cycle under the temperature and photoexcitation are the same (Table 1), despite the presence of double bonds in the structure. The geometry of molecules in the excited state is indicative of the possibility of opening of the strained tetratomic cycle with the retained hexatomic cycle in the structure (Fig. 3 III-c, III-d). The breaking of the single bond at the opening of the cycle without additional interaction with other substances (air components) can lead to the electron density redistribution and formation of a double bond in the monocyclic molecule.

The calculation showed that in 3S-caren (Fig. 3 III-e, III-f), both the photo- and temperature excitations lead to the lengthening of the C3-C6 bond included in the hexatomic and triatomic cycles (Table 1). The bond length increases under photoexcitation by 0.308 A, which is noticeably smaller than in the molecules with the tetratomic and hexatomic cycles. At the opening of the tetratomic cycle in the previously investigated compounds, the hexatomic cycle was retained, while the breaking of the C3-C6 bond in 3S-caren should lead to the formation of the heptatomic cycle in the excited state (Fig. 3 III-f). The atomic structure of a molecule in the excited state can return to the initial state; therefore, despite the growth of the C3-C6 bond length, the initial structure will, most probably, be retained.

Due to the presence of strained cycles [35], many terpene compounds tend to the thermal isomerization. The temperature transformations are accompanied by the opening of the tetratomic cycle or tetratomic and hexatomic cycles simultaneously. Figure 4b shows a schematic of the thermal decomposition [35] and Fig. 4a, a calculated schematic of the atomic structure variation.

According to the calculation, in the alpha-pinene molecule both under the photo- and temperature excitation, the single C6-C7 bond length increases (under photoexcitation, by 1.194 A). Thus, the experimental data on the thermal isomerization of a molecule caused by the bond breaking and opening of the tetratomic cycle are consistent with the data obtained using the technique of determination of the KS of molecules at high temperatures.
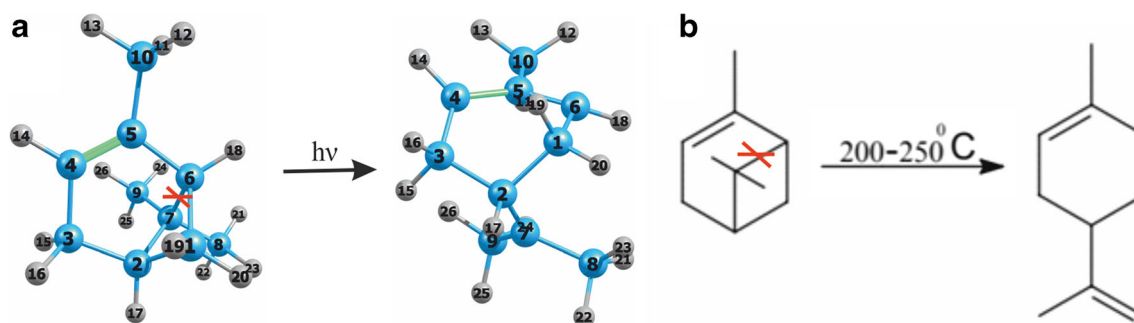

Fig. 4 Isomerization of the alpha-pinene molecule: (**a**) calculated data and (**b**) data from [35]

Conclusions

Analysis of the terpene molecules is of great importance for ecology, since these molecules represent pest insect pheromones, and, in addition, can be used in the perfumery industry. Using the quantum chemical methods, we studied the excited state and calculated the bond vibrations for the organic molecules containing the strained cycles and conjugated, double, and single bonds. We estimated the effect of temperature on the atomic structure by the kinetic stability technique. The approaches used allowed us to estimate the stability of molecules against solar radiation and temperature. The temperature excitation of the unsaturated acyclic and monocyclic compounds will, most probably, change the single bond lengths, while the photoexcitation affects first the multiple bonds and leads to their elongation. In the unsaturated bicyclic terpenes, the photo- and temperature excitations lead to the analogous structural transformations, specifically, to the probable breaking of the single bond included in both cycles and opening of the tetratomic cycle at the retained hexatomic one. The analogous thermal isomerization reaction in the alpha-pinene molecule was described in the literature, which confirms the reliability of the calculated data. Thus, there are two possible parallel mechanisms of deactivation of the calculated molecules: under solar radiation and under the action of temperature.

Our analysis can be interesting for ecological application, since it allows, first, estimating the stability of pheromones and, second, predicting the features of chemical communication of insects. Since for the species searching for a mate at night time, i.e., at low temperatures and minimum electromagnetic radiation intensity, the pheromone molecules can start decomposing in the beginning of the daylight under the action of, i.e., UV radiation, and continue decomposing with an increase in the air temperature during the day, the concentration of molecules by the next night will be minimum. The characteristic lifetime of pheromone molecules of the insects searching for a mate during the daytime, i.e., at the strong electromagnetic radiation and high air temperature, can be short. This can limit the radius of attraction of mates to the insects producing pheromones. Thus, the characteristic lifetime of pheromone molecules will determine the mechanism of pheromone search and the type of molecules that can be used as pheromones.

References

1. Regnier FE, Law JH (1968) Insect pheromones. J Lipid Res 9(5): 541–551

2. Buser H-R, Guerin PM, Tóth M, Szöcs G, Schmid A, Francke W, Arn H (1985) (Z,Z)-6,9-nonadecadien-3-one and (Z,Z,Z)-3,6,9-nonadecatriene: identification and synthesis of sex pheromone components of Peribatodes rhomboidaria. Tetrahedron Lett 26:403–406

3. Pajares JA, Alvarez G, Ibeas F et al (2010) Identification and field activity of a male-produced aggregation pheromone in the pine sawyer beetle, Monochamus galloprovincialis. J Chem Ecol 36(6):570–583

4. Lei H, Chiu H-Y (2013) Responses of protocerebral neurons in Manduca sexta to sex-pheromone mixtures. J Comp Physiol A 199(11):997–1014

5. Tomilin FN, Osina OV, Kuzubov AA et al (2011) Stability of forest lepidopteran pheromones against environmental factors. Biophysics 4:714–722

6. Shi R-W, Liu F (2016) Quantum chemical study on the stability of honeybee queen pheromone against atmospheric factors. J Mol Model 22:140

7. Soukhovolsky VG, Tomilin FN, Artyushenko PV, Tsikalova PE (2016) System of Forest insect pheromone communication: stability of «information» molecules to environmental factors. Siberian. J For Sci 3:67–76

8. Soukhovolsky VG, Volkova (Tsikalova) PE, Tarasova OV (2014) Modeling of forest insect pheromone communication system. Female as a Source of Information, Siberian. J For Sci 6:69–79

9. Artyushenko PV, Tomilin FN, Ovchinnikov SG et al (2017) The stability of the pheromones of xylophagous insects to environmental factors: an evaluation by quantum chemical analysis. Biophysics 62:532–538

10. Fedorov AS, Fedorov DA, Kuzubov AA, Avramov PV, Nishimura Y, Irle S, Witek HA (2011) Relative isomer abundance of fullerenes and carbon nanotubes correlates with kinetic stability. Phys Rev Lett 107:175506

11. Fedorov AS, Kuzubov AA, Visotin MA, Tomilin FN (2017) New method for calculations of nanostructure kinetic stability at high temperature. J Magn Magn Mater 440:167–170

12. Lee C, Yang W, Parr RG (1988) Development of the Colle-Salvetti correlation-energy formula into a functional of the electron density. Phys Rev B 37:785–789

13. Becke AD (1988) Density-functional exchange-energy approximation with correct asymptotic behavior. Phys Rev A 38:3098–3100

14. Miehlich B, Savin A, Stoll H, Preuss H (1989) Results obtained with the correlation energy density functionals of Becke and Lee-Yang and Parr. Chem Phys Lett 157:200–206

15. Schmidt MW, Baldridge KK, Boatz JA, Elbert ST, Gordon MS, Jensen JH, Koseki S, Matsunagaetal N (1993) General atomic and molecular electronic structure system. Comput Chem 14:1347–1363

16. Runge E, Gross EKU (1984) Density-functional theory for time-dependent systems. Phys Rev Lett 52-12:997–1000

17. Petersilka M, Gossmann U, Gross EKU (1996) Excitation energies from time-dependent density-functional theory. Phys Rev Lett 76-8: 1212–1215

18. Curtiss LA, Raghavachari K, Redfern PC, Pople JA (1997) Assessment of Gaussian-2 and density functional theories for the computation of enthalpies of formation. J Chem Phys 106(3):1063–1068

19. Curtiss LA, Redfern PC, Raghavachari K (2005) Assessment of Gaussian-3 and test set of experimental energies. J Chem Phys 123:124107–124119

20. Tirado-Rives J, Jorgensen WL (2008) Performance of B3LYP density functional methods for a large set of organic molecules. J Chem Theory Comput 4:297–306

21. Fredj D, Hassen CB, Elleuch S, Feki H, Boudjada NC, Mhiri T, Boujelbene M (2017) Structural, vibrational and optical properties of a new organic–inorganic material: (C5H8N3)2[BiCl5], J. Mater Res Bull 85:23–29

22. Schuchardt KL, Didier BT, Elsethagen T, Sun L, Gurumoorthi V, Chase J, Li J, Windus TL (2007) Basis set exchange: a community database for computational sciences. J Chem Inf Model 47-3:1045–1052

23. Feller D (1996) The role of databases in support of computational chemistry calculations. J Comput Chem 17-13:1571–1586

24. Artyushenko PV, Tomilin FN, Kuzubov AA, Ovchinnikov SG, Tsikalova PE, Ovchinnikova TM, Soukhovolsky VG (2016) Action of the atomic and electronic structure of pheromone molecules on the effectiveness of communication in xylophagous insects. J Struct Chem 57(2):287–293

25. Nesmeyanov AN, Nesmeyanov NA (1974) Organic chemistry. Chemistry, Moscow

26. Kirk RE, Othmer DF (1983) Encyclopedia of chemical technology 223rd edn. Wiley, New York

27. Breitmaier E (2006) Terpenes: flavors, fragrances, pharmaca, pheromones. Willey-VCH, Weinheim

28. Birgersson G, Schlyter F, Löfqvist J et al (1984) Quantitative variation of pheromone components in the spruce bark beetle Ips typographus from different attack phases. J Chem Ecol 10:1029–1055

29. Pettersson E, Boland W (2003) Potential parasitoid attractants, volatile composition throughout a bark beetle attack. Chemoecology 13:27–37

30. Fan J, Kang L, Sun J (2007) Role of host volatiles in mate location by the Japanese pine sawyer, Monochamus alternatus hope (Coleoptera: Cerambycidae). Environ Entomol 36:58–63

31. Allison JD, Borden JH, McIntosh RL et al (2001) Kairomonal response by four Monochamus species (Coleoptera: Cerambycidae) to bark beetle pheromones. J Chem Ecol 27:633–647

32. Nabil N (2009) State of the art on the monitoring of the pine wood nematode –PWN (Bursaphelenchusxylophilus) and its insect vector (Monochamusgalloprovincialis) in Europe. Institut Européen de la forêtcultivée EFIATLANTIC, Cestas

33. Ibeas F, Diez JJ, Pajares JA (2008) Olfactory sex attraction and mating behaviour in the pine sawyerMonochamus galloprovincialis (Coleoptera: Cerambycidae). J Insect Behav 21:101–111

34. Ibeas F, Gallego D, Diez JJ et al (2007) An operative kairomonal lure for managing pine sawyer beetle Monochamus galloprovincialis (Coleoptera: Cerymbycidae). J Appl Entomol 131:13–20

35. Plemenkov VV (2007) Khimiya izoprenoidov (the chemistry of isoprenoids). Izd. Altais. Univer, Barnaul